

trans-N-(Heterocyclic Carbene) Platinum(II)

Acetylide Chromophores as Phosphors for OLED Applications

James D. Bullock[§], Zhengtao Xu[†], Silvano Valandro[†], Muhammad Younus^{†*},
Jiangeng Xue^{†*} and Kirk S. Schanze^{†,*}

[§]Department of Chemistry, University of Florida, P.O. Box 117200, Gainesville, FL 32611

[†]Department of Materials Science and Engineering, University of Florida, Gainesville, FL 32611

[†]Department of Chemistry, University of Texas at San Antonio, San Antonio, TX 78249

email: kirk.schanze@utsa.edu, jxue@mse.ufl.edu, muhammad.younus@utsa.edu

Abstract

A family of complexes of the type *trans*-(NHC)₂Pt(C≡C-Ar)₂ (NHC = N-heterocyclic carbene and Ar = substituted phenyl or 4-pyridyl) exhibits blue or blue-green phosphorescence. The photoluminescence is 10 – 50 fold more efficient when the materials are in dispersed in a solid poly(methyl methacrylate) glass compared to in THF solution. The phosphorescence quantum efficiencies in PMMA glass range from 0.20 – 0.65, varying with the structure of the aryl acetylide ligands. Organic light emitting diodes (OLEDs) were fabricated by thermal evaporation, using

bis[2-(diphenylphosphino)phenyl] ether oxide (DPEPO) as the host and 15% of the *trans*-(NHC)₂Pt(C≡C-Ar)₂ complexes as the dopant/emitters. Most of the OLEDs display good performance, with EL spectra that closely match the PL in the PMMA glass. The best performing materials have peak EQE ranging from 9.6 – 14.1%, with deep blue spectral profiles (minimum CIE (0.16,0.13). Several of the complexes have deep HOMO levels and they display poor EL performance attributed to inefficient host to emitter hole transfer.

Keywords

OLED, phosphor, blue emission, platinum N-heterocyclic carbene, platinum acetylide

Introduction

Since the first report of a convenient synthetic route,¹⁻³ platinum acetylide⁴⁻⁷ molecules, oligomers and polymers have been considered as model organometallic complexes in photophysics⁸⁻¹² for fundamental investigation of triplet excited states in π -conjugated materials. In addition, studies have explored potential applications of platinum acetylides in phosphorescent organic light emitting diodes (OLED),¹³⁻¹⁶ solar cells,¹⁷⁻²⁰ and as nonlinear absorption chromophores.²¹⁻²⁵ Platinum acetylide materials are air stable, have good thermal stability, and are soluble in common organic solvents, properties which render them processible from solution and by vacuum thermal deposition. One reason for the interest in platinum acetylide materials is fundamental investigation and application of triplet states in organic electronics.^{8, 12, 16} Excitation of these complexes is accompanied by rapid singlet \rightarrow triplet intersystem crossing that affords triplet excitons in high yield.^{16, 26} In some cases the polymers⁹ and complexes²⁷ exhibit moderate to high room temperature phosphorescence yields. However, in many systems long triplet lifetimes and low phosphorescence quantum yields limit their application as active materials in OLEDs.²⁸

The σ -donor (and π -acceptor) long chain alkyl phosphines induces the structural distortions in the excited states, leading to the thermal deactivation via low-lying d-d states.²⁹

During the past several decades, research efforts have been made to regulate the frontier orbitals of the platinum complexes to minimize the non-radiative decay pathways of their excited states. New platinum-containing phosphorescent chromophores were obtained by using multi-dentate ligands.^{28, 30-31} The strong donor ability, and rigid molecular structure in the excited and ground states of these materials results in high emission quantum yields.³⁰ Applying this concept, a series of red³²⁻³³ and green³⁴ phosphorescent complexes were reported recently. However, reports on the development of deep blue platinum-based phosphorescent chromophores are rare.^{28, 30, 32, 35-37} Compared to platinum complexes based on multi-dentate ligands, complexes that feature N-heterocyclic carbene (NHC) ligands have shown great ability to produce efficient blue phosphorescent emitters.^{28, 30, 38-39} Strong σ -donor and weak π -acceptor NHC ligands⁴⁰ form a strong bond with platinum, thus destabilizing the d-d excited state manifold, resulting in a decrease of non-radiative decay and an increase radiative decay via phosphorescence.⁴¹ Inclusion of heterocyclic carbene in the tetra-dentate ligands, and their complexation with platinum give rise to deep blue phosphorescent chromophores.³⁰

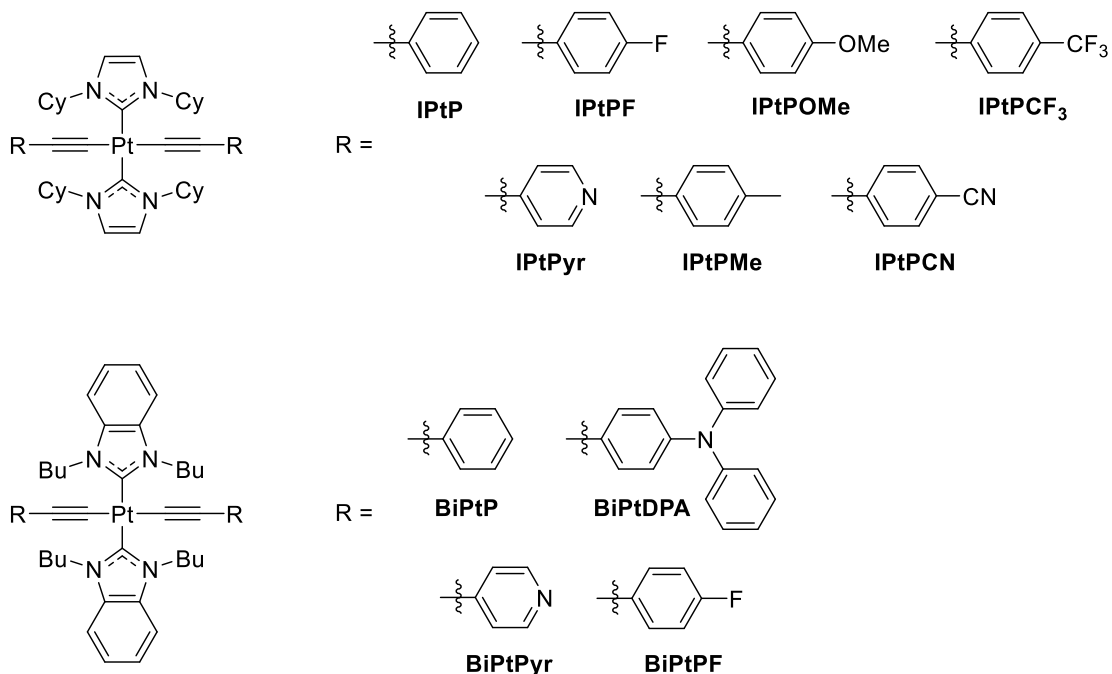


Chart 1. Structures and acronyms for the *trans*-NHC Platinum(II) acetylide complexes.

Reproduced with permission from Ref. 29. Copyright 2019 ACS Publications.

Recently, a family of complexes of the type *trans*-(NHC)₂Pt(C≡C-Ar)₂ was reported by our group (Chart 1).^{29, 42} This new family of complexes is constructed using *trans*-N-heterocyclic carbene ligands instead of alkyl phosphines which are often used as auxiliary ligands in platinum acetylide complexes.⁴² The NHC-based complexes feature moderate to efficient room temperature phosphorescence depending on the structure of the aryl acetylide ligands.²⁹ Previously reported analogous complexes with phosphine ligands also exhibit phosphorescence, but only at low temperature, demonstrating the advantage of the NHC ligands. Photophysical measurements on solid state PMMA films of platinum acetylide complex IPtP (Chart 1) displayed phosphorescence quantum yield of 0.30, giving a narrow deep blue photoluminescence with CIE coordinates of (0.14, 0.12). Furthermore, an OLED device fabricated with IPtP as the emitter features a maximum external quantum efficiency of 7.8% with CIE coordinates of (0.20, 0.20).⁴³

In this work, we report the solid state photophysics and OLED device performance of the previously reported family *trans*-(NHC)₂Pt(C≡C-Ar)₂ complexes with variation of NHC and acetylidy ligands (Chart 1).²⁹ First, the photophysical properties of the complexes doped into a solid state poly(methyl methacrylate) (PMMA) matrix were investigated. The results show that in the solid-state, the complexes' phosphorescence quantum yields and triplet lifetimes are substantially greater than those in solutions. These results are a manifestation of substantially reduced non-radiative decay rates in the solid state. Second, the family of complexes were used as emitters in OLED devices; many of the chromophores display good performance with external quantum efficiency up to 14 % and CIE color coordinates of (0.16, 0.13). However, several complexes with high phosphorescence yields in solid state display poor performance in the OLEDs. Electrochemical studies indicate that these latter complexes have very deep highest occupied molecular orbital (HOMO) levels giving rise to inefficient hole transfer from the host.

Experimental Section

Materials. Platinum complexes IPtP, IPtPF, IPtPOMe, IPtPCF₃, IPtPyr, IPtPMe, IPtPCN, BiPtP, BiPtDPA, BiPtPyr and BiPtPF were prepared as previously reported.²⁹

Steady State and Time Resolved Photoluminescence Measurements. For solid-state samples, the chromophore was mixed into a PMMA stock solution (16 mg/mL PMMA in chlorobenzene, 2 wt% chromophore), and the resulting solution was drop cast onto glass slides (1 cm × 2.5 cm). Steady-state photoluminescence measurements were performed on a Horiba Fluorolog-3 spectrophotometer with xenon arc lamp and Horiba photomultiplier tube (detector range: 290-850 nm) modified with a petite integrating sphere. When the excitation beam was characterized, a 14% neutral density filter was used to attenuate the light going to the detector. In

a separate experiment, the filter was characterized at the excitation wavelength to determine the correction factor.

Phosphorescence lifetimes of the solid-state samples were recorded with a PicoQuant FluoTime 300 Fluorescence Lifetime Spectrophotometer by the time-correlated single photon counting (TCSPC) technique. A Ti:sapphire Coherent Chameleon Ultra laser was used as excitation source. The Chameleon laser provides pulses of 80 MHz that can be tuned from 680-1080 nm. The 80 MHz pulse train was sampled using a Coherent Model 9200 pulse picker to provide excitation pulses at an acceptable repetition rate and was frequency doubled using a Coherent second harmonic generator. An excitation wavelength of 340 nm was chosen for all samples.

OLED Fabrication and Device Testing. OLED fabrication and device testing were performed according to methods reported previously.⁴⁴⁻⁴⁵ The devices were fabricated on glass substrates commercially precoated with a layer of indium tin oxide (ITO) with a sheet resistance of ~15 Ω/sq. The substrates were cleaned with soapy water, deionized water, acetone, and isopropanol consecutively, and then exposed to ultraviolet ozone for 15 min immediately before loading into a high-vacuum deposition chamber (background pressure lower than 4 x 10⁻⁶ Torr). 4,4'- Cyclohexylidenebis[N,N-bis(4-methylphenyl) benzenamine] (TAPC) (30 nm thick), *tris*(4-carbazoyl-9-ylphenyl)amine (TCTA) (10 nm), *bis*[2-(diphenylphosphino)phenyl] ether oxide (DPEPO): 15% emitter (20nm), DPEPO (10nm), 2,2',2''-(1,3,5-benzinetriyl)-*tris*(1-phenyl-1-H-benzimidazole) (TPBi) (30 nm), LiF (1 nm) and aluminum cathode (100 nm) were deposited in succession without breaking the vacuum (see below for device stack schematic and Chart S1 in SI

for chemical structures of materials). A crossbar geometry was used for the patterned ITO anode and the Al cathode, which defined an active device area of 4 mm².

The electroluminescence spectra of the OLEDs were obtained using an Ocean Optics spectrometer (USB 2000) and a Keithley 2400 power source. Current-density-voltage (J-V) characteristics of the devices were measured using an Agilent 4155C semiconductor parameter analyzer under ambient conditions. The luminance was calculated from the photocurrent of a calibrated silicon detector (Newport 818 UV) that was placed close to the devices assuming Lambertian emission. The external quantum efficiencies were then calculated from luminance and device spectra.

Electrochemical Characterization. Cyclic voltammetry was acquired using a CHI 760E electrochemical workstation with 2 mm diameter platinum working electrode, Ag/Ag⁺ reference electrode, and platinum wire counter electrode. The complexes were dissolved in dry CH₂Cl₂ to a concentration of ~1 mM, and mixed with 0.1 M tetra-n-butylammonium hexafluorophosphate (nBu₄PF₆) and then purged with argon for 20 minutes. Experiments were then conducted under argon with a scan rate of 100 mV/s.

Results and Discussion

The platinum acetylide chromophores were doped into a polymethyl methacrylate (PMMA) matrix at 2 wt% and the emission spectrum, emission quantum yield and lifetime were measured for each solid sample. The solid state photophysical properties for the family of complexes are shown in Table 1, including the CIE color coordinates for each chromophore. (A full characterization of the photophysical properties of the family of complexes in THF solution, including absorption, emission and transient absorption is provided in our earlier study.²⁹) In general, the solid-state emission spectra are consistent with those previously reported in THF solution,²⁹ showing the same

peak and vibronic shoulder. On the basis of the previous study and the lifetimes (μ s timescale), the emission is attributed to phosphorescence from the triplet state. Notably, the solid-state emission quantum yields for all of the complexes are moderate to high (0.2 – 0.6 range), and the values are significantly larger than for the same complexes in solution. The lifetimes range from ~ 10 – 50 μ s and they are also significantly higher in the solid matrix compared to solution.^{29, 43} Interestingly, there are two complexes that are exceptions: IPtPCN and BiPtPDPA feature emission quantum yields and lifetimes and that are consistent between solution and solid state. The trans-(NHC)₂Pt(C≡C-Ar)₂ complexes have been reported to possess a non-emissive d-d excited state that lies just above the emitting ($^3\pi, \pi^*$) state.²⁹ Note that these two complexes have the lowest energy emission,²⁹ and these similar photophysical properties between solution and solid state suggest that the d-d state is not thermally accessible for IPtPCN and BiPtPDPA because the emitting state is too low in energy. This provides insight into the mechanism for the enhanced emission for the other complexes in the PMMA solid state matrix.

Table 1. Photophysical Properties of NHC Pt(II) Acetylides in PMMA Glass

Complex	λ_{max} / nm	CIE	$\Phi_{\text{PMMA}} (\Phi_{\text{THF}})^a$	$\tau_{\text{PMMA}} (\tau_{\text{THF}})^b / \mu\text{s}$
IPtP	442	(0.14, 0.12)	0.30 (0.029)	9 (1.7)
IPtPMe	442	(0.15, 0.17)	0.35 (0.065)	22 (3.7)
IPtPF	436	(0.15, 0.15)	0.47 (0.04)	22 (2.1)
IPtPyr	432	(0.14, 0.10)	0.65 (0.012)	17 (0.10)
IPtPCN	483	(0.21, 0.47)	0.42 (0.45)	45 (39)
IPtPOMe	441	(0.15, 0.17)	0.47 (0.06)	25 (1.1)
IPtPCF ₃	452	(0.15, 0.20)	0.44 (0.19)	23 (5)
BiPtP	438	(0.14, 0.12)	0.56 (0.08)	21 (1.8)
BiPtPyr	431	(0.14, 0.09)	0.58 (0.012)	16 (0.35)
BiPtPF	435	(0.15, 0.12)	0.45 (0.06)	24 (1.4)

BiPtPDPA	483	(0.21, 0.49)	0.22 (0.12)	34 (36)
----------	-----	--------------	-------------	---------

^a Quantum yield values in THF solution (from ref 29). ^b Lifetime values in THF solution (from ref 29) Comparison between solution and solid-state rate radiative and non-radiative decay rate constants (k_r and k_{nr} , respectively) is provided in SI (Table S1). Interestingly, the radiative rates remain similar between the solid and solution, generally staying within a factor of two of each other. By contrast, the non-radiative decay rates are 10 – 50 times lower in the solid state compared to in solution. Note that IPtPCN and BiPtPDPA, which have the lowest triplet-energy exhibit the smallest difference in the non-radiative decay rates for solution and the solid state. In our previous report,²⁹ it was hypothesized that for the *trans*-(NHC)₂Pt(C≡C-Ar)₂ complexes the dominant non-radiative decay pathway was via a thermally activated crossing to a non-emissive metal centered (d-d) excited state which lies energetically above the emissive $^3\pi,\pi^*$ state that is responsible for the phosphorescence. Taken together, the photophysical results here suggest that crossing to the d-d state is suppressed in the solid state, giving rise to the higher phosphorescence quantum yields.⁴⁶

The solid PMMA matrix is a rigid environment so the fact that access to the d-d state¹² is suppressed implies that there is a significant change in the geometry of the emitter in the excited

state. One explanation for this is that access to the d-d state is accompanied by out-of-plane distortion of the square planar configuration of the complex. This theory is supported by TDDFT calculations for a platinum(II) acetylide complex with a tridentate ligand.⁴⁶ Zhang et al. observed an enhancement of the emission quantum yield from the dichloromethane solution to the solid film (10 wt% emitter in PMMA host) of similar blue light emitting N-heterocyclic carbene acetylide complexes that resulted for the increased rigidity and weaker internuclear interactions in solid state.⁴¹

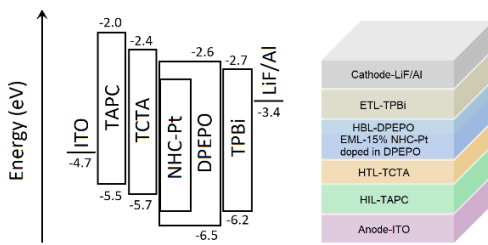


Figure 1. OLED device structure and energy scheme (in eV)

Organic Light-Emitting Diode Characterization. OLEDs were constructed using each of the *trans*-(NHC)₂Pt(C≡C-Ar)₂ as the dopant/emitter. The device structure used is shown in Figure 1, and it was the same as previously reported for the IPtP complex:⁴³ indium-tin oxide (ITO) /4,4'-cyclohexylidenebis[N,N-bis(4-methylphenyl) benzenamine] (TAPC) (30 nm)/ tris(4-carbazoyl-9-ylphenyl)amine (TCTA) (10 nm)/bis[2-(diphenylphosphino)phenyl] ether oxide (DPEPO): 15% dopant (20 nm)/ DPEPO (10 nm)/2,2',2''-(1,3,5-benzenetriyl)-*tris*(1-phenyl-1-*H*-benzimidazole) (TPBi) (30 nm)/LiF (1 nm)/Al (100nm). The emitters were included at 15% in DPEPO based on optimization studies in which IPtP was doped in DPEPO at levels ranging from 5 – 20%, with 15% giving the highest efficiency.⁴³ The OLED device characterization and performance for all of the devices/materials are listed in Table 2. A comparison of the electroluminescence (EL) and photoluminescence (PL) spectra and optoelectronic device performance characteristics for

selected devices/materials are provided in Figure 2, and the same for the remaining complexes are shown in the supporting information.

Table 2. OLED Device Performance

Complex	$\lambda_{\text{max}}/\text{nm}$	CIE_{EL}	CIE_{PL}	EQE_{max}	EQE (100 cd/m ²)
IPtP	441	(0.20, 0.20)	(0.14, 0.12)	7.8%	4.1%
IPtPF	439	(0.16, 0.14)	(0.15, 0.15)	10.1%	5.9%
IPtPyr	396	(0.25, 0.19)	(0.14, 0.10)	0.8%	0.78%
IPtPOMe	444	(0.16, 0.16)	(0.15, 0.17)	9.6%	5.0%
IPtPCF ₃	457	(0.17, 0.19)	(0.15, 0.20)	2.1%	1.4%
IPtPCN	489	(0.21, 0.49)	(0.21, 0.47)	1.9%	0.97%
BiPtP	439	(0.16, 0.13)	(0.14, 0.12)	14.1%	10.2%
BiPtPyr	391	(0.29, 0.23)	(0.14, 0.09)	0.7%	0.6%
BiPtPF	436	(0.17, 0.14)	(0.15, 0.12)	10.5%	6.0%

As can be seen from the data, most of the devices with the *trans*-(NHC)₂Pt(C≡C-Ar)₂ complexes as the dopant/emitters exhibit EL spectra with similar band maxima and bandshape compared to the solid-state PL spectra. However, there are some important differences in OLED efficiency for the different dopant/emitters, and notably some of the OLEDs performed poorly. First, on the positive side, the device that employed BiPtP as the emitter showed the best performance with a peak 14% EQE and CIE color coordinates of (0.16, 0.13), which is very close to the photoluminescence CIE color coordinates of (0.14, 0.12) and that of the National Television Systems Committee CIE color coordinate for ideal blue (0.14, 0.08). OLEDs based on the IPtPOMe, IPtPF, and BiPtPF emitters also showed good peak EQEs and good deep blue color purity. Unfortunately, all of the efficient devices exhibited significant efficiency roll-off at luminance above 100 cd/m². The efficiency roll-off likely arises from triplet-triplet annihilation and triplet-carrier quenching due to the relatively long triplet lifetimes of the family of complexes.

More disappointing was the observation that devices with several emitters that displayed high PL quantum efficiency did not perform well in EL devices. Notable among this set are the emitters IPtPCF₃, IPtPCN, IPtPyr and BiPtPyr. These four complexes share a common feature of containing the pyridine aryl unit or phenyl substituted with a strongly electron withdrawing group. Insight into the poor OLED performance comes from the EL spectra of IPtPCN, IPtPyr and BiPtPyr (SI Figures S1 and S3), which exhibit significant contribution of a high energy emission feature at $\lambda_{\text{max}} \sim 400$ nm that is due to emission from the hole transport layer or exciplex at the interface. This observation suggests that there is inefficient hole transfer from the host to the emitter, due to a relatively deep HOMO on the emitter (see below). In any case, the result was surprising considering the high PL quantum yields observed for the pyridine-based Pt-acetylides complexes. It is possible that further device optimization and/or use of different host and hole transport materials could allow optimization of OLEDs with the set of emitters that gave poor EL efficiency.

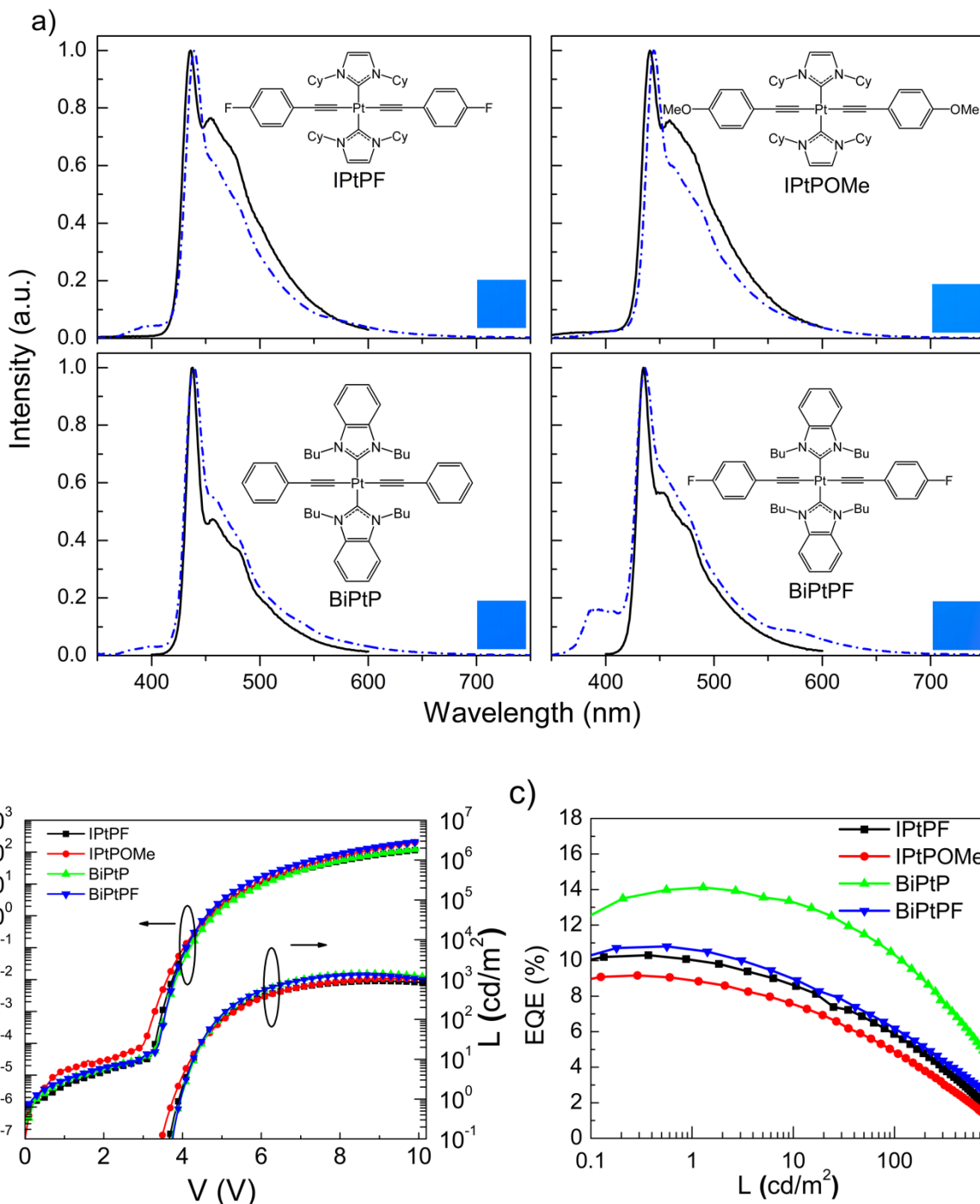


Figure 2. a) Photoluminescence (black/solid line) comparison to electroluminescence (blue/dash-dot line); b) Voltage vs current and luminance characteristics; c) Luminance vs EQE for IPtPF, IPtPOMe, BiPtP, and BiPtPF. Color patches in a) simulate the EL color based on the CIE coordinates which are calculated from the EL spectral distributions.

Electrochemistry. In order to better assess the device electronic properties and explain the varying OLED emitter efficiencies, electrochemistry was carried out on the *trans*-(NHC)₂Pt(C≡C-Ar)₂ complexes by using cyclic voltammetry (CV) in CH₂Cl₂ solution. The CV allowed us to estimate the HOMO levels of the complexes, which are related to the efficiency of hole transfer from the DPEPO host. All of the complexes exhibited one or more anodic waves that were irreversible, with the exception of IPtPOMe, which displayed one reversible and second quasi-reversible wave (SI Figures S6 and S7). The onset values for the anodic waves are listed in Table 3, along with estimated HOMO energy levels. Also included in the table is the data for the host DPEPO which was measured under the same conditions as the complexes.

Table 3. Electrochemical Data and Estimated HOMO Energy Levels.

Compound	E _{ox} ^{onset} / V ^a	E _{HOMO} / eV ^c
IPtPOMe	0.37 ^b	-5.17
IPtP	0.54	-5.34
IPtPF	0.57	-5.37
BiPtP	0.65	-5.45
BiPtPF	0.71	-5.51
IPtPCN	0.75	-5.55
IPtPCF ₃	0.76	-5.56
DPEPO	1.54	-6.34
BiPtPyr	1.57	-6.37
IPtPyr	1.58	-6.38

^a Measured value is onset of irreversible anodic wave, potential vs. Fc/Fc⁺ in CH₂Cl₂/ 0.1 M NBu₄PF₆. ^b Quasi-reversible anodic wave.
^c E_{HOMO} = -(4.8 + E_{ox}^{onset}).⁴⁷

Notable is the fact that for most of the complexes the HOMO levels are significantly higher (less negative) compared to the HOMO of the DPEPO host. This signals that host to emitter hole transfer is expected to be efficient. Note that the trend is for the HOMO levels to shift to more negative values with increasing electron withdrawing strength of the substituents. Most evident is the fact that the two pyridine-based emitters (IPtPyr and BiPtPyr) feature HOMO levels that are

below (more negative) compared to the estimated level for DPEPO. This finding confirms the expectation based on the OLED results, which suggested that hole transfer from the host to the pyridine-based emitters may be inefficient.

General Discussion. In previous work we demonstrated that a family of carbene complexes of the type *trans*-(NHC)₂Pt(CC-Ar)₂ display moderately efficient phosphorescence in the deep blue spectral region in solution at ambient temperatures.²⁹ The emission arises from a triplet excited state that is mainly based on the aryl acetylid ligands, with a small contribution from a metal-to-ligand charge transfer configuration (e.g., $^3\pi,\pi^*$ with small $^3\text{MLCT}$ contribution). The previous work also demonstrated that the phosphorescence becomes considerably more efficient at low temperatures in a rigid solvent glass.²⁹ Analysis of temperature dependent photophysical data suggested that the enhanced phosphorescence at low temperatures arises due to suppression of a thermally activated crossing to a metal centered (d-d) state which acts as a funnel facilitating non-radiative decay of the emissive $^3\pi,\pi^*$ state. The current study shows that the same family of complexes displays very efficient phosphorescence at ambient temperatures in a polymer glass matrix at room temperature. This finding suggests that crossing to the d-d state from the emissive state is suppressed in the solid state due to a rigidochromic effect,⁴⁸ whereby the $^3\pi,\pi^* \rightarrow \text{d-d}$ transition requires a distortion of the complex's geometry that is constrained in the PMMA matrix.

28, 30, 41

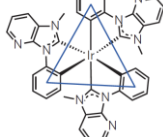
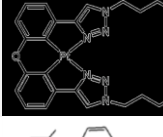
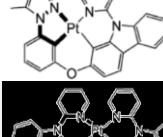
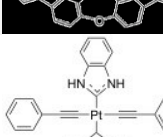
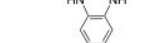
Given the efficient phosphorescence for the *trans*-(NHC)₂Pt(CC-Ar)₂ complexes in the solid state, it is reasonable to assume that the chromophores could serve as emitters for deep blue OLEDs. The current study bears this out, notably in OLED device applications four of the complexes display quite efficient, deep blue emissions with peak EQE > 9.5%. Table 4 below compares the solid state photophysical properties and OLED parameters for some of the most

efficient deep blue phosphors based on Ir(III) or Pt(II) complexes that have been reported in the literature. While there is some disparity in the experimental conditions, there are interesting comparisons to be drawn. First, in the previous work, the most efficient Ir(III)-based phosphors are complexes with bidentate C-donor ligands where one of the units is an N-heterocyclic carbene. By contrast, for the Pt(II) systems, the most efficient phosphors are based on tetra-dentate, N,C-donor ligands that provide a rigid, square planar environment. The emission color (based on CIE coordinates) and peak EQE for the BiPtP NHC phosphor is competitive with the other Ir(III) and Pt(II) emitters; however, as noted above the NHC phosphors reported herein suffer from significant efficiency roll-off at higher luminance. The comparison in Table 4 makes the origin of this effect clear: the emission lifetime of BiPtP is 5 – 20 fold longer than the other Ir(III) and Pt(II) phosphors. The significantly longer lifetime in the NHC systems must arise due to relatively weaker spin-orbit coupling in the emissive excited state, which is a manifestation of the fact that the emitting state is largely $^3\pi,\pi^*$, with relatively small contribution of Pt-based orbitals.^{29, 49} By contrast, the other the Ir(III) and Pt(II) phosphors emit from excited states that have a greater MLCT contribution and consequently more metal-based d-orbital contribution to the emissive excited states. This gives rise to greater spin-orbit coupling, which enhances the radiative and non-radiative decay rates.

Also notable in the results is the fact that the pyridine-based emitters, IPtPyr and BiPtPyr display the most efficient photoluminescence quantum yields, but both complexes give poor device performance. IPtPCF₃ and IPtPCN also display relatively low EQE, despite having relatively high photoluminescence yields. The low efficiency for the pyridine complexes may be related to their deep HOMO levels leading to inefficient hole-transfer from the DPEPO host. The IPtPCF₃ and IPtPCN complexes have higher HOMO levels, suggesting that hole transfer from DPEPO should

be facile. In these cases we do not have the explanation for the low device efficiency, but it could be related to imbalance in the rate of hole and electron transfer to the dopants. Nevertheless, this study did not attempt to fully optimize the structure of the OLEDs tested, including varying the host or hole transporting material. It is quite likely that with further materials and device engineering OLEDs based on these complexes can be optimized and may give rise to higher efficiencies and deep blue emission.

Table 4. Deep Blue OLED Phosphors

Complex	ϕ_{PL}^a	τ_{PL}^a	EQE_{max}^b	EQE_{100}^c	CIE ^d	REF
	0.75	$\sim 1 \mu S$	13.4	12.5	(0.15, 0.05)	⁵⁰
	0.76	1.2	10.1	9.0 ^e	(0.16, 0.09)	⁵¹
	0.58	5	15.4	12.3	(0.15, 0.17)	⁵²
	0.85	4.5	25.2	23.3	(0.15, 0.13)	³⁷
	0.83	3.8	21.2	9.7	(0.15, 0.21)	⁵³
	0.56	21	14.1	10.2	(0.16, 0.13)	this work

^a Photophysical parameters in solid state (either 77 K glass or polymer matrix at 298 K). ^b OLED external quantum efficiency at maximum. ^c OLED external quantum efficiency at 100 cd/m². ^d CIE 1931 color coordinates. ^e Measured at 1000 cd/m².

Conclusions

A series of blue OLEDs were fabricated using phosphorescent *trans*-N-(heterocyclic carbene) platinum(II) acetylide chromophores as active materials. First, photophysical investigations were performed that demonstrate higher PL quantum yield and increased triplet lifetime in solid state (in PMMA matrices) compared to those in fluid solution (in THF). The strong σ -donor carbenes destabilize the excited d-d state which reduces thermal population (nonradiative decay). Furthermore, access to the d-d state is suppressed in the solid PMMA matrices due to the increased rigidity and weaker internuclear interactions. High quantum yield (0.2-0.6) emissions in the blue spectral region and microsecond lifetime made these materials good candidates for blue OLEDs.

OLED devices were fabricated and characterized using the blue emitters with the variation of carbenes (with imidazole and benzimidazole backbone) and acetylides (with substituted phenyl and 4-pyridyl substituents) to optimize the EQE and color purity. Among the emitters, benzimidazole containing chromophore BiPtP showed the best performance in the deep blue with a peak 14% EQE and CIE color coordinates of (0.16, 0.13). The OLEDs based on the IPtPOME (EQE: 9.6%; CIE: 0.16, 016) IPtPF (EQE: 10.1%; CIE: 0.16, 014), and BiPtPF (EQE: 10.5%; CIE: 0.17, 014) emitters also showed good EQEs and deep blue color purity. Nevertheless, all of these devices exhibited significant efficiency roll-off at luminance above 100 cd/m² due to triplet-triplet annihilation and triplet-carrier quenching for relatively long triplet lifetimes.

Devices made from the emitters with pyridyl aryl acetylide (IPtPyr and BiPtPyr) and phenyl acetylide with strong electron withdrawing substituents (IPtPCF₃, IPtPCN) displayed poor performance despite their high PL quantum yield (0.44-0.65). High energy emission bands in the EL spectra suggested emissions from the hole transport layer resulting insufficient hole transfer

from the host to the emitter. The deeper HOMO levels of these emitters compared to the host material (DPEPO) are responsible for inadequate hole transfer.

In conclusion, the N-(heterocyclic carbene) platinum(II) phosphors offer new possibilities to design and fabricate deep blue OLEDs. Judicious choice of carbenes and acetylide in the phosphors can increase the quantum yield and decrease triplet exciton lifetime that would be suitable for OLEDs with deep blue color purity, high EQEs and small efficiency roll-off.

Supporting Information

Photophysical (photoluminescence and electroluminescence spectra), electrochemical (CV) and OLED characterization plots (voltage vs current and luminance, and luminance vs EQE) of platinum complexes *trans*- IPtP, IPtPF, IPtPOMe, IPtPCF₃, IPtPyr, IPtPMe, IPtPCN, BiPtP, BiPtDPA, BiPtPyr and BiPtPF are available.

Acknowledgements

This work was supported by the National Science Foundation (Grant Nos. CHE-1737714 and CHE-1904288). K.S.S. also acknowledges the Welch Foundation for support through the Welch Chair at the University of Texas at San Antonio (Award No. AX-0045-20110629). J.X. and Z.X. acknowledge partial support by the National Science Foundation (Grant Nos. CHE-1507561 and CHE-1904534).

References

1. Sonogashira, K.; Yatake, T.; Tohda, Y.; Takahashi, S.; Hagihara, N., Novel Preparation of s-Alkynyl Complexes of Transition-Metals by Copper(II) Iodide-Catalyzed Dehydrohalogenation. *J. Chem. Soc. Chem. Commun.* **1977**, (9), 291-292.
2. Sonogashira, K.; Fujikura, Y.; Yatake, T.; Toyoshima, N.; Takahashi, S.; Hagihara, N., Syntheses and Properties of cis-Dialkynyl and trans-Dialkynyl Complexes of Platinum(II). *J. Organomet. Chem.* **1978**, *145* (1), 101-108.
3. Sonogashira, K.; Ohga, K.; Takahashi, S.; Hagihara, N., Studies of Poly-yne Polymers Containing Transition-Metals in the Main Chain .6. Synthesis of Nickel-Poly-yne Polymers by Alkynyl Ligand-Exchange Using a Copper(II) Catalyst. *J. Organomet. Chem.* **1980**, *188* (2), 237-243.
4. Haque, A.; Al-Balushi, R. A.; Al-Busaidi, I. J.; Khan, M. S.; Raithby, P. R., Rise of Conjugated Poly-ynes and Poly(Metalla-ynes): From Design Through Synthesis to Structure–Property Relationships and Applications. *Chem. Rev.* **2018**, *118* (18), 8474-8597.
5. Long, N. J.; Williams, C. K., Metal Alkynyl σ Complexes: Synthesis and Materials. *Angew. Chem.* **2003**, *42* (23), 2586-2617.
6. Wong, W.-Y.; Ho, C.-L., Di-, Oligo- and Polymetallaynes: Syntheses, Photophysics, Structures and Applications. *Coord. Chem. Rev.* **2006**, *250* (19), 2627-2690.
7. Ho, C.-L.; Yu, Z.-Q.; Wong, W.-Y., Multifunctional Polymetallaynes: Properties, Functions and Applications. *Chem. Soc. Rev.* **2016**, *45* (19), 5264-5295.
8. Silverman, E. E.; Cardolaccia, T.; Zhao, X. M.; Kim, K. Y.; Haskins-Glusac, K.; Schanze, K. S., The Triplet state in Pt-Acetylide Oligomers, Polymers and Copolymers. *Coord. Chem. Rev.* **2005**, *249* (13-14), 1491-1500.

9. Wilson, J. S.; Chawdhury, N.; Al-Mandhary, M. R. A.; Younus, M.; Khan, M. S.; Raithby, P. R.; Kohler, A.; Friend, R. H., The Energy Gap Law for Triplet States in Pt-Containing Conjugated Polymers and Monomers. *J. Am. Chem. Soc.* **2001**, *123* (38), 9412-9417.
10. Cooper, T. M.; Krein, D. M.; Burke, A. R.; McLean, D. G.; Rogers, J. E.; Slagle, J. E.; Fleitz, P. A., Spectroscopic Characterization of a Series of Platinum Acetylide Complexes Having a Localized Triplet Exciton. *J. Phys. Chem. A* **2006**, *110* (13), 4369-4375.
11. Köhler, A.; Wilson, J., Phosphorescence and Spin-Dependent Exciton Formation in Conjugated Polymers. *Org. Electron.* **2003**, *4* (2), 179-189.
12. Rogers, J. E.; Hall, B. C.; Hufnagle, D. C.; Slagle, J. E.; Ault, A. P.; McLean, D. G.; Fleitz, P. A.; Cooper, T. M., Effect of Platinum on the Photophysical Properties of a Series of Phenyl-Ethynyl Oligomers. *J. Chem. Phys.* **2005**, *122* (21), 214708.
13. Ho, C.-L.; Chui, C.-H.; Wong, W.-Y.; Aly, S. M.; Fortin, D.; Harvey, P. D.; Yao, B.; Xie, Z.; Wang, L., Efficient Electrophosphorescence from a Platinum Metallocopolyne Featuring a 2,7-Carbazole Chromophore. *Macromol. Chem. Phys.* **2009**, *210* (21), 1786-1798.
14. Lu, W.; Mi, B.-X.; Chan, M. C. W.; Hui, Z.; Che, C.-M.; Zhu, N.; Lee, S.-T., Light-Emitting Tridentate Cyclometalated Platinum(II) Complexes Containing σ -Alkynyl Auxiliaries: Tuning of Photo- and Electrophosphorescence. *J. Am. Chem. Soc.* **2004**, *126* (15), 4958-4971.
15. Xu, L.-J.; Zeng, X.-C.; Wang, J.-Y.; Zhang, L.-Y.; Chi, Y.; Chen, Z.-N., Phosphorescent PtAu₂ Complexes with Differently Positioned Carbazole-Acetylide Ligands for Solution-Processed Organic Light-Emitting Diodes with External Quantum Efficiencies of over 20%. *ACS Appl. Mater. Interfaces* **2016**, *8* (31), 20251-20257.

16. Wilson, J. S.; Dhoot, A. S.; Seeley, A.; Khan, M. S.; Kohler, A.; Friend, R. H., Spin-Dependent Exciton Formation in pi-Conjugated Compounds. *Nature* **2001**, *413* (6858), 828-831.

17. Wong, W.-Y.; Ho, C.-L., Organometallic Photovoltaics: A New and Versatile Approach for Harvesting Solar Energy Using Conjugated Polymetallaynes. *Acc. Chem. Res.* **2010**, *43* (9), 1246-1256.

18. Mei, J.; Ogawa, K.; Kim, Y.-G.; Heston, N. C.; Arenas, D. J.; Nasrollahi, Z.; McCarley, T. D.; Tanner, D. B.; Reynolds, J. R.; Schanze, K. S., Low-Band-Gap Platinum Acetylide Polymers as Active Materials for Organic Solar Cells. *ACS Appl. Mater. Interfaces* **2009**, *1* (1), 150-161.

19. Zhao, X.; Piliego, C.; Kim, B.; Poulsen, D. A.; Ma, B.; Unruh, D. A.; Fréchet, J. M. J., Solution-Processable Crystalline Platinum-Acetylide Oligomers with Broadband Absorption for Photovoltaic Cells. *Chem. Mater.* **2010**, *22* (7), 2325-2332.

20. Guo, F.; Ogawa, K.; Kim, Y.-G.; Danilov, E. O.; Castellano, F. N.; Reynolds, J. R.; Schanze, K. S., A Fulleropyrrolidine End-Capped Platinum-Acetylide Triad: the Mechanism of Photoinduced Charge Transfer in Organometallic Photovoltaic Cells. *Phys. Chem. Chem. Phys.* **2007**, *9* (21), 2724-2734.

21. Shelton, A. H.; Valandro, S. R.; Price, R. S.; Dubinina, G. G.; Abboud, K. A.; Wicks, G.; Rebane, A.; Younus, M.; Schanze, K. S., Stereochemical Effects on Platinum Acetylide Two-Photon Chromophores. *J. Phys. Chem. A* **2019**, *123* (43), 9382-9393.

22. Rogers, J. E.; Slagle, J. E.; Krein, D. M.; Burke, A. R.; Hall, B. C.; Fratini, A.; McLean, D. G.; Fleitz, P. A.; Cooper, T. M.; Drobizhev, M.; Makarov, N. S.; Rebane, A.; Kim, K.-Y.;

Farley, R.; Schanze, K. S., Platinum Acetylide Two-Photon Chromophores. *Inorg. Chem.* **2007**, *46* (16), 6483-6494.

23. Dubinina, G. G.; Price, R. S.; Abboud, K. A.; Wicks, G.; Wnuk, P.; Stepanenko, Y.; Drobizhev, M.; Rebane, A.; Schanze, K. S., Phenylene Vinylene Platinum(II) Acetylides with Prodigious Two-Photon Absorption. *J. Am. Chem. Soc.* **2012**, *134* (47), 19346-19349.

24. Zieba, R.; Desroches, C.; Chaput, F.; Carlsson, M.; Eliasson, B.; Lopes, C.; Lindgren, M.; Parola, S., Preparation of Functional Hybrid Glass Material from Platinum (II) Complexes for Broadband Nonlinear Absorption of Light. *Adv. Funct. Mater.* **2009**, *19* (2), 235-241.

25. Shelton, A. H.; Price, R. S.; Brokmann, L.; Dettlaff, B.; Schanze, K. S., High Efficiency Platinum Acetylide Nonlinear Absorption Chromophores Covalently Linked to Poly(methyl methacrylate). *ACS Appl. Mater. Interfaces* **2013**, *5* (16), 7867-7874.

26. Ramakrishna, G.; Goodson, T.; Rogers-Haley, J. E.; Cooper, T. M.; McLean, D. G.; Urbas, A., Ultrafast Intersystem Crossing: Excited State Dynamics of Platinum Acetylide Complexes. *J. Phys. Chem. C* **2009**, *113* (3), 1060-1066.

27. Pomestchenko, I. E.; Luman, C. R.; Hissler, M.; Ziessel, R.; Castellano, F. N., Room Temperature Phosphorescence from a Platinum(II) Diimine Bis(pyrenylacetylide) Complex. *Inorg. Chem.* **2003**, *42* (5), 1394-1396.

28. Li, K.; Cheng, G.; Ma, C.; Guan, X.; Kwok, W.-M.; Chen, Y.; Lu, W.; Che, C.-M., Light-Emitting Platinum(II) Complexes Supported by Tetridentate Dianionic bis(N-heterocyclic carbene) Ligands: Towards Robust Blue Electrophosphors. *Chem. Sci.* **2013**, *4* (6), 2630-2644.

29. Bullock, J. D.; Valandro, S. R.; Sulicz, A. N.; Zeman, C. J.; Abboud, K. A.; Schanze, K. S., Blue Phosphorescent trans-N-Heterocyclic Carbene Platinum Acetylides: Dependence on Energy Gap and Conformation. *J. Phys. Chem. A* **2019**, *123* (42), 9069-9078.

30. Fleetham, T.; Li, G.; Li, J., Phosphorescent Pt(II) and Pd(II) Complexes for Efficient, High-Color-Quality, and Stable OLEDs. *Adv. Mater.* **2017**, *29* (5), 1601861.

31. Haque, A.; Xu, L.; Al-Balushi, R. A.; Al-Suti, M. K.; Ilmi, R.; Guo, Z.; Khan, M. S.; Wong, W.-Y.; Raithby, P. R., Cyclometallated Tridentate Platinum(II) Arylacetylide Complexes: Old Wine in New Bottles. *Chem. Soc. Rev.* **2019**, *48*, 5547-5563.

32. Vezzu, D. A. K.; Deaton, J. C.; Jones, J. S.; Bartolotti, L.; Harris, C. F.; Marchetti, A. P.; Kondakova, M.; Pike, R. D.; Huo, S., Highly Luminescent Tetradentate Bis-Cyclometalated Platinum Complexes: Design, Synthesis, Structure, Photophysics, and Electroluminescence Application. *Inorg. Chem.* **2010**, *49* (11), 5107-5119.

33. Velusamy, M.; Chen, C.-H.; Wen, Y. S.; Lin, J. T.; Lin, C.-C.; Lai, C.-H.; Chou, P.-T., Cyclometalated Platinum(II) Complexes of Lepidine-Based Ligands as Highly Efficient Electrophosphors. *Organometallics* **2010**, *29* (17), 3912-3921.

34. Tam, A. Y.-Y.; Tsang, D. P.-K.; Chan, M.-Y.; Zhu, N.; Yam, V. W.-W., A Luminescent Cyclometalated Platinum(II) Complex and its Green Organic Light Emitting Device with High Device Performance. *Chem. Commun.* **2011**, *47* (12), 3383-3385.

35. Murphy, L.; Brulatti, P.; Fattori, V.; Cocchi, M.; Williams, J. A. G., Blue-Shifting the Monomer and Excimer Phosphorescence of Tridentate Cyclometallated Platinum(II) Complexes for Optimal White-Light OLEDs. *Chem. Commun.* **2012**, *48* (47), 5817-5819.

36. Fleetham, T.; Wang, Z.; Li, J., Efficient Deep Blue Electrophosphorescent Devices Based on Platinum(II) bis(n-methyl-imidazolyl)benzene Chloride. *Org. Electron.* **2012**, *13* (8), 1430-1435.

37. Hang, X.-C.; Fleetham, T.; Turner, E.; Brooks, J.; Li, J., Highly Efficient Blue-Emitting Cyclometalated Platinum(II) Complexes by Judicious Molecular Design. *Angew. Chem.* **2013**, *52* (26), 6753-6756.

38. Li, T.-Y.; Liang, X.; Zhou, L.; Wu, C.; Zhang, S.; Liu, X.; Lu, G.-Z.; Xue, L.-S.; Zheng, Y.-X.; Zuo, J.-L., N-Heterocyclic Carbenes: Versatile Second Cyclometalated Ligands for Neutral Iridium(III) Heteroleptic Complexes. *Inorg. Chem.* **2015**, *54* (1), 161-173.

39. Zhang, Y.; Hauke, C. E.; Crawley, M. R.; Schurr, B. E.; Fulong, C. R. P.; Cook, T. R., Increasing Phosphorescent Quantum yields and lifetimes of platinum-alkynyl complexes with extended conjugation. *Dalton Trans.* **2017**, *46* (30), 9794-9800.

40. Bourissou, D.; Guerret, O.; Gabbaï, F. P.; Bertrand, G., Stable Carbenes. *Chem. Rev.* **2000**, *100* (1), 39-92.

41. Zhang, Y.; Blacque, O.; Venkatesan, K., Highly Efficient Deep-Blue Emitters Based on cis and trans N-Heterocyclic Carbene PtII Acetylide Complexes: Synthesis, Photophysical Properties, and Mechanistic Studies. *Chem. Eur. J.* **2013**, *19* (46), 15689-15701.

42. Winkel, R. W.; Dubinina, G. G.; Abboud, K. A.; Schanze, K. S., Photophysical Properties of trans-Platinum Acetylide Complexes Featuring N-Heterocyclic Carbene Ligands. *Dalton Trans.* **2014**, *43* (47), 17712-17720.

43. Bullock, J. D.; Salehi, A.; Zeman, C. J.; Abboud, K. A.; So, F.; Schanze, K. S., In Search of Deeper Blues: Trans-N-Heterocyclic Carbene Platinum Phenylacetylide as a Dopant for Phosphorescent OLEDs. *ACS Appl. Mater. Interfaces* **2017**, *9* (47), 41111-41114.

44. Zheng, Y.; Eom, S.-H.; Chopra, N.; Lee, J.; So, F.; Xue, J., Efficient Deep-Blue Phosphorescent Organic Light-Emitting Device with Improved Electron and Exciton Confinement. *App. Phys. Lett.* **2008**, *92* (22), 223301.

45. Yang, Y.; Cohn, P.; Eom, S.-H.; Abboud, K. A.; Castellano, R. K.; Xue, J., Ultraviolet-Violet Electroluminescence from Highly Fluorescent Purines. *J. Mater. Chem. C* **2013**, *1* (16), 2867-2874.

46. Lam, W. H.; Lam, E. S.-H.; Yam, V. W.-W., Computational Studies on the Excited States of Luminescent Platinum(II) Alkynyl Systems of Tridentate Pincer Ligands in Radiative and Nonradiative Processes. *J. Am. Chem. Soc.* **2013**, *135* (40), 15135-15143.

47. Cardona, C. M.; Li, W.; Kaifer, A. E.; Stockdale, D.; Bazan, G. C., Electrochemical Considerations for Determining Absolute Frontier Orbital Energy Levels of Conjugated Polymers for Solar Cell Applications. *Adv. Mater.* **2011**, *23* (20), 2367-2371.

48. Lees, A. J., The Luminescence Rigidochromic Effect Exhibited by Organometallic Complexes: Rationale and Applications. *Comments Inorg. Chem.* **1995**, *17* (6), 319-346.

49. Glusac, K.; Köse, M. E.; Jiang, H.; Schanze, K. S., Triplet Excited State in Platinum–Acetylide Oligomers: Triplet Localization and Effects of Conformation. *J. Phys. Chem. B* **2007**, *111* (5), 929-940.

50. Pal, A. K.; Krotkus, S.; Fontani, M.; Mackenzie, C. F. R.; Cordes, D. B.; Slawin, A. M. Z.; Samuel, I. D. W.; Zysman-Colman, E., High-Efficiency Deep-Blue-Emitting Organic Light-Emitting Diodes Based on Iridium(III) Carbene Complexes. *Adv. Mater.* **2018**, *30* (50), 1804231.

51. Lee, J.; Chen, H.-F.; Batagoda, T.; Coburn, C.; Djurovich, P. I.; Thompson, M. E.; Forrest, S. R., Deep Blue Phosphorescent Organic Light-Emitting Diodes with Very High Brightness and Efficiency. *Nat. Mater.* **2016**, *15* (1), 92-98.

52. Wang, X.; Peng, T.; Nguyen, C.; Lu, Z.-H.; Wang, N.; Wu, W.; Li, Q.; Wang, S., Highly Efficient Deep-Blue Electrophosphorescent Pt(II) Compounds with Non-Distorted Flat Geometry: Tetradentate versus Macrocyclic Chelate Ligands. *Adv. Funct. Mater.* **2017**, *27* (4), 1604318.

53. Fleetham, T. B.; Huang, L.; Klimes, K.; Brooks, J.; Li, J., Tetradentate Pt(II) Complexes with 6-Membered Chelate Rings: A New Route for Stable and Efficient Blue Organic Light Emitting Diodes. *Chem. Mater.* **2016**, *28* (10), 3276-3282.

TOC Graphic

